

Resource and Mobility Management in Hybrid LiFi and WiFi Networks: A User-Centric Learning Approach

Han Ji, *Student Member, IEEE*, Xiping Wu, *Senior Member, IEEE*

Abstract—Hybrid light fidelity (LiFi) and wireless fidelity (WiFi) networks (HLWNets) are an emerging indoor wireless communication paradigm, which combines the advantages of the capacious optical spectra of LiFi and ubiquitous coverage of WiFi. Meanwhile, load balancing (LB) becomes a key challenge in resource management for such hybrid networks. The existing LB methods are mostly network-centric, relying on a central unit to make a solution for the users all at once. Consequently, the solution needs to be updated for all users at the same pace, regardless of their moving status. This would affect the network performance in two aspects: i) when the update frequency is low, it would compromise the connectivity of fast-moving users; ii) when the update frequency is high, it would cause unnecessary handovers as well as hefty feedback costs for slow-moving users. Motivated by this, we investigate user-centric LB which allows users to update their solutions at different paces. The research is developed upon our previous work on adaptive target-condition neural network (ATCNN), which can conduct LB for individual users in quasi-static channels. In this paper, a deep neural network (DNN) model is designed to enable an adaptive update interval for each individual user. This new model is termed as mobility-supporting neural network (MSNN). Associating MSNN with ATCNN, a user-centric LB framework named mobility-supporting ATCNN (MS-ATCNN) is proposed to handle resource management and mobility management simultaneously. Results show that at the same level of average update interval, MS-ATCNN can achieve a network throughput up to 215% higher than conventional LB methods such as game theory, especially for a larger number of users. In addition, MS-ATCNN costs an ultra low runtime at the level of 100s μ s, which is two to three orders of magnitude lower than game theory.

Index Terms—Light fidelity (LiFi), wireless fidelity (WiFi), hybrid network, load balancing, resource allocation, mobility management, deep neural network (DNN), machine learning

I. INTRODUCTION

ON the road to the sixth generation (6G) communication systems, hybrid light fidelity (LiFi) and wireless fidelity (WiFi) networks (HLWNets) are an emerging paradigm of indoor wireless technologies [1]. LiFi operates in a way similar to WiFi but on the vast visible light spectrum (400-790 THz), offering remarkable advantages including license-free, electromagnetic interference-free, high physical layer security, etc [2]. Recent experimental work shows that LiFi

can provide a link data rate of 24 Gbps over a single light-emitting diode chip [3]. In addition, LiFi can be integrated into the existing lighting infrastructure and provide illumination and communication simultaneously, rendering energy-saving potentials. Meanwhile, LiFi faces the challenges of light-path blockage caused by opaque objects such as human bodies and furniture [4], despite the non-line-of-sight (NLoS) paths can facilitate the data transmission to some extent [5]. Also, LiFi offers a relatively small coverage area with a single access point (AP), usually around a few metres in diameter. In contrast, the WiFi AP gives a larger coverage range (up to 50 meters) but a lower throughput, which achieved 92 Mbps in average by 2023 [6]. The complementary advantages of LiFi and WiFi motivate the co-existence of them in the indoor wireless systems, composing HLWNets which have gained increasing attention in recent years [7]. Such hybrid networks can significantly improve the network capacity over stand-alone LiFi or WiFi networks [8].

In HLWNets, the coverage of LiFi and WiFi APs overlaps each other, imposing a great challenge in terms of AP selection. Signal strength strategy (SSS), which selects the AP that provides the highest received signal power for the user equipment (UE), is widely employed in homogeneous networks where the coverage overlap is restricted among APs. In this scenario, load balancing (LB) is optional when the traffic loads are distributed unevenly in geography, and it only applies to the cell-edge UEs which are covered by more than one AP. However, severe traffic imbalance could occur when the SSS method is applied to hybrid networks [9], even though the traffic loads are distributed evenly in geography. As a result, the effectiveness of SSS is drastically compromised, while LB becomes an essential and challenging resource management issue in HLWNets.

Another significant challenge that is faced by HLWNets is the mobility management. For a mobile UE, handovers are necessary to transfer it from one AP to another, in order to maintain a decent link quality. There are two basic types of handovers for hybrid networks: i) horizontal handover (HHO), which takes place between two APs of the same type; and ii) vertical handover (VHO), which occurs between different types of APs. Due to the relatively small coverage of LiFi APs, the HHOs within LiFi could be very frequent for fast-moving UEs, compromising their wireless connectivity. Unlike HHOs, VHOs are usually caused by the demands for LB. Since the LB solution of one UE is affected by other UEs, frequent VHOs might still occur when the UE is moving slow or even

The work of H. Ji is supported by the China Scholarship Council (Grant No. 202106620012). X. Wu acknowledges the support of the Charlemount Grant by Royal Irish Academy (RIA). *Corresponding author: Xiping Wu*

H. Ji and X. Wu are with the School of Electrical and Electronic Engineering, University College Dublin, Dublin, D04 V1W8, Ireland (e-mail: han.ji@ucdconnect.ie; xiping.wu@ucd.ie).

TABLE I
SUMMARY OF RELATED WORK. (✓: SUPPORTED, ✗: NOT SUPPORTED, NA: NOT APPLICABLE)

Ref.	Envir.	Method	Load balancing	User-centric	Update Interval	Complexity
[10]	Quasi-static	Global optimisation	✓	✗	NA	Extremely high
[11]		Game theory	✓	✗		High
[12]		College admission model	✓	✗		Low
[13]		Fuzzy logic	✓	✗		Medium
[14]		Mixed fuzzy logic and optim.	✓	✗		Ultra low
[15], [16]		Reinforcement learning	✓	✗		
[17]		Deep neural network	✓	✓		
[18]	Mobile	Decomposition-based optim.	✓	✗	Fixed (500ms)	High
[19]		College admission model	✓	✗	Fixed	
[20]		Fuzzy logic	✓	✗	Fixed	Low
[21]		Handover skipping	✗	✓	Fixed TTT (160ms)	Ultra low
[22]		ANN-aided handover	✗	✓	Fixed TTT (160ms)	
[23]		ANN-aided handover	✗	✓	Fixed TTT (2s)	
This work		Deep neural network	✓	✓	Adaptive	

static. This makes the mobility management become a tricky issue for HLWNets, particularly in conjunction with the LB problem stated above.

A. Related Work

1) *Load Balancing in a Quasi-Static Environment*: The LB problem is comprised of two sub-problems for the UE: i) selection of the host AP and ii) resource allocation of the host AP. A joint optimisation problem is often formulated to address this issue, by establishing a mathematical model between the input (e.g., channel quality, traffic demands, quality of service (QoS) requirements, etc.) and the output (i.e., AP selection and resource allocation). So far, a considerable number of studies have been carried out to investigate LB for HLWNets in a quasi-static environment [10]–[17]. Depending on how the mathematical model is constructed, the noted works can be classified into two broad categories: i) physical model-based methods and ii) machine learning-based methods. The former category consists of global optimisation, iterative algorithms, and rule-based algorithms. Among them, global optimisation [10] and iterative algorithms [11], [12] can reach an optimal (or near-optimal) solution at the cost of exceeding computational complexity. To lower the processing power, rule-based algorithms such as fuzzy logic [13] were reported to make a direct decision on the LB solution, sacrificing the optimality to some extent. In [14], a compound method that mixes fuzzy logic and optimisation was proposed to enhance the algorithm’s optimality. Nevertheless, this method is still sub-optimal as well as sensitive to network deployment.

In contrast to the physical model-based methods, machine learning-based methods can better balance optimality and complexity, at the expense of a training process. A few efforts have been made to explore reinforcement learning for solving the LB issue [15], [16]. Though these methods can achieve satisfactory optimality with low complexity, they would need to retrain the models when the UE number varies, greatly limiting its practicability. In our previous work [17], a deep neural

network (DNN) based method named adaptive target-condition neural network (ATCNN) was proposed, with a unique feature of determining the LB solution for a single target UE. The scheme also involves an adaptive mechanism that can map any smaller number of UEs to a preset number, without affecting the LB decision for the target UE. As a result, ATCNN can tackle the LB problem for various UE numbers without the need for retraining. In addition, the ATCNN method can achieve near-optimal network performance with an ultra-low implementation runtime in sub-milliseconds [17].

2) *Load Balancing in a Mobile Environment*: The above papers all consider a quasi-static environment, where the LB decision is made upon invariant channel knowledge. In a mobile environment, however, the handover process is necessary to transfer the UE from one AP to another. To apply the aforementioned LB methods for time-varying channels, the corresponding algorithms must be recalculated to update the AP selection decision regularly. However, most of the existing LB methods are network-centric, e.g., [10]–[16]. In other words, they rely on a central unit to make the LB decisions for all UEs at the same time. Consequently, the LB decisions need to be updated at the same pace for all UEs, regardless of their moving status which might be very distinctive in practice. Some UEs could move relatively fast while others could be slow or even static. For fast-moving UEs, a high update frequency is necessary to retain strong connectivity to the host AP. Meanwhile, slow-moving UEs might experience unnecessary feedback costs as well as frequent handovers with a high update frequency. While a few relevant studies have considered a mobile environment [18]–[20], the contradictory demands for update frequency cannot be intrinsically met by the network-centric LB methods.

A handful of handover schemes have been studied for HLWNets, from the perspective of user-centric rather than network-centric [21]–[23]. In [21], the authors amended the standard handover scheme of the 3rd generation partnership project (3GPP) to realise handover skipping, which can ef-

effectively suppress frequent handovers in HLWNets. Several learning-aided approaches have also been developed on this topic. In [22], an artificial neural network (ANN) model was built to decide the host AP through balancing multiple factors including channel quality, resource availability, and UE mobility. A similar work was carried out in [23], except that the handover decision was constructed as a binary classification problem, which determines whether the UE should be transferred to a target AP or stay with the current host AP. Unlike the LB methods [18], [19], [24] carrying out a centralised style of decision-making, the handover schemes [21]–[23] make the decision for each individual UE separately, while a fixed time-to-trigger (TTT) is usually adopted. As a result, these handover schemes can well support the various moving status of individual UEs. However, they fail to render the crucial capability of LB, leading to a less efficient use of network resources. The related works aforementioned are summarised in Table I. To the best knowledge of the authors, no LB approach has yet been developed to address the distinctive demands for update frequency among the mobile UEs.

B. Contribution

In this paper, a novel user-centric learning approach is developed to tackle the challenging LB issue in a mobile environment. The proposed method is constructed on the basis of our previous work ATCNN [17], which embraces a unique property of user-centric LB. In this work, the update interval of ATCNN is modelled to be adjustable for each individual UE, upon both its link status and moving status. The aim is to acquire a suitable update interval for the individual UE, bridging the needs for resource management and mobility management. The main contribution of this work is three-fold:

- A DNN model is developed to determine the update interval for an individual UE, with four inputs related to the UE: the current host AP, link quality, movement direction and speed. A throughput-degradation criterion is defined for collecting the ground-truth labels of update interval, which allows the UE throughput to reduce by a certain percentage against an ideal case where the update interval is infinitesimal. This criterion reflects a trade-off between the demands for LB and mobility. The proposed DNN model, which is referred to as mobility-supporting neural network (MSNN), enables the update interval to adapt to the UE moving status.
- A mobility-supporting LB framework is built, which interconnects ATCNN and the proposed MSNN. This framework is termed as mobility-supporting ATCNN (MS-ATCNN). In general, ATCNN and MSNN form an iterative loop: i) ATCNN determines the host AP for an individual UE and forwards this information to MSNN; and ii) MSNN decides an update interval for implementing ATCNN in the next time. It is worth noting that there is no error propagation in the iterative process, since both outputs of ATCNN and MSNN depend on the current status of the UE. The proposed MS-ATCNN enables the UEs to update their LB solutions at different paces in a mobile environment.

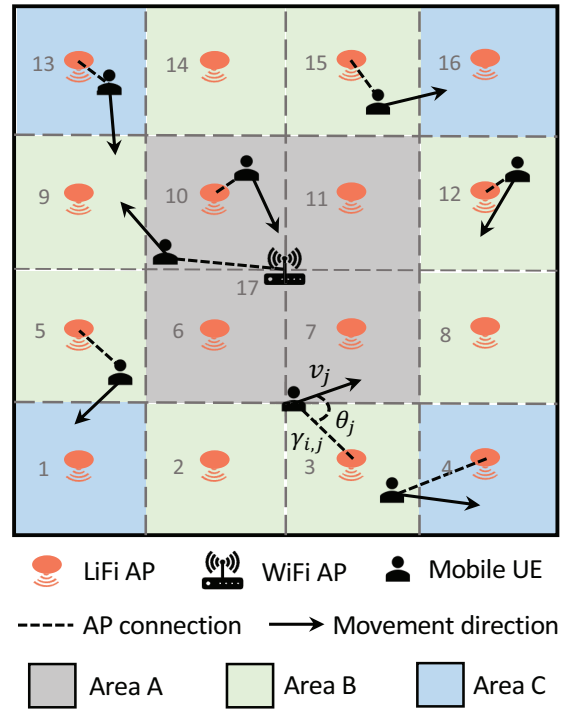


Fig. 1. Schematic diagram of an indoor HLWNet (top view).

- The learning model performance of MS-ATCNN is investigated, including ablation studies to verify its effectiveness. Also, the wireless network performance of MS-ATCNN is analysed in a mobile environment, in comparison with several baseline methods including: i) ATCNN without MSNN, ii) conventional network-centric LB methods (such as game theory (GT)), and iii) straightforward AP selection methods without the capability of LB (such as SSS). Results show that MSNN can boost the throughput of ATCNN by up to 38%, against the case without MSNN. In comparison to GT and SSS, MS-ATCNN can improve the throughput by up to 215% and 310%, respectively.

The remainder of this paper is organised as follows. The system model of HLWNet is introduced in Section II. The proposed method is presented in Section III, including the MSNN model, the MS-ATCNN framework, the criterion for sample data collection, and the process of training and test. Ablation studies of MS-ATCNN are carried out in Section IV. Simulation results are presented in Section V. Finally, conclusions are drawn in Section VI.

II. SYSTEM MODEL

The system model of HLWNets in a mobile environment is introduced in this section, including the network model, the channel model, and the mobility model.

A. Network Model

The network topology of the HLWNet considered in this paper is presented in Fig. 1, which consists of 16 LiFi APs

and 1 WiFi AP. The LiFi APs are arranged in a grid on the ceiling, while the WiFi AP is located at the centre of the room on the floor. According to the geographic symmetry, the LiFi APs can be divided into 3 areas, which are marked with different colours in Fig 1. Details about this division will be explained in Section III-A. The UEs move around in the room with random initial positions, which are assumed to be uniformly distributed. Let N_a and N_u denote the number of APs and the number of UEs; let $\mathbb{S} = \{1, 2, \dots, N_a\}$ and $\mathbb{U} = \{1, 2, \dots, N_u\}$ denote the set of APs and the set of UEs; let i and j denote the index of APs and the index of UEs, where $i \in \mathbb{S}$ and $j \in \mathbb{U}$, respectively. Each UE has a certain data rate requirement, which is denoted by R_j . The data rate requirements across the UEs are assumed to follow a Gamma distribution with unity shape parameter. Let a binary variable $\chi_{i,j}$ indicate the connection status of the link between AP i and UE j , then $\chi_{i,j} = 1$ means that UE j is connected to AP i , and otherwise $\chi_{i,j} = 0$. Each UE is served by one and only one AP, which each AP can serve multiple UEs via time-division multiple access. The proportion of time that AP i allocates to UE j is denoted by $\rho_{i,j}$, which is a continuous variable in the range between 0 and 1.

B. Channel Model

The LiFi channel is usually comprised of two components: line-of-sight (LoS) and non-line-of-sight (NLoS) paths. We refer interested readers to [14] for a detailed channel model of LiFi, while the channel model of WiFi used in this paper can be found in [13]. The signal-to-noise ratio (SNR) of the link between AP i and UE j is denoted by $\gamma_{i,j}$, of which the math expressions can be found in [14, eq. (5)] for LiFi and [13, eq. (7)] for WiFi. The corresponding link capacity, which is denoted by $C_{i,j}$, can be expressed as follows [17, eq. (1)]:

$$C_{i,j} = \begin{cases} \frac{B_i}{2} \log_2 \left(1 + \frac{e}{2\pi} \gamma_{i,j} \right), & \forall i \in \mathbb{S}_{\text{LiFi}} \\ B_i \log_2 (1 + \gamma_{i,j}), & \forall i \in \mathbb{S}_{\text{WiFi}} \end{cases}, \quad (1)$$

where e is the Euler's number; B_i denotes the bandwidth of AP i ; \mathbb{S}_{LiFi} is the set of LiFi APs; \mathbb{S}_{WiFi} is the set of WiFi APs, despite only one WiFi AP is considered in this paper.

C. Mobility Model

Random waypoint (RWP) [25] is a widely used synthetic mobility model. With the RWP model, UE j moves along a zigzag path, from one point $P_j^{(l)}$ to the next point $P_j^{(l+1)}$. These waypoints are uniformly distributed in the room area. Let $\theta_j^{(l)}$ represent the angle between the UE's movement direction and the line that connects the UE to its host AP, as demonstrated in Fig. 1. During the excursion from $P_j^{(l)}$ to $P_j^{(l+1)}$, the UE moves at a random speed $v_j^{(l)}$, which follows a uniform distribution within the range $(0, v_{\max}]$, where v_{\max} denotes the maximum speed. The average speed of all UEs is given by $\bar{v} = E[v_j]$. The movement of UE leads to a time-varying channel and hence a time-varying link capacity. Let $C_{i,j}^{(t)}$ denote the link capacity between AP i and UE j at time instance t . Similarly, we define $\rho_{i,j}^{(t)}$ and $\chi_{i,j}^{(t)}$. The

instantaneous throughput achieved by the j -th UE at time t is denoted by $\Gamma_j^{(t)}$, which can be calculated by:

$$\Gamma_j^{(t)} = \sum_{i \in \mathbb{S}} \rho_{i,j}^{(t)} \chi_{i,j}^{(t)} C_{i,j}^{(t)}. \quad (2)$$

III. PROPOSED METHOD FOR RESOURCE AND MOBILITY MANAGEMENT

In this section, the proposed MSNN model is elaborated, followed by an introduction to the framework of MS-ATCNN, which interconnects MSNN and ATCNN to jointly tackle the resource and mobility management. Then the throughput-degradation criterion is introduced for collecting the sample dataset of update intervals. Finally, we present the process of training, validation, and test.

A. Mobility-Support Neural Network (MSNN)

The MSNN model aims to yield an update interval that suits the mobile UE, based on its status including the SNR, movement direction, and speed. These variables are denoted by γ_k , θ_k , and v_k , respectively, where k denotes the target UE. The output is a single variable T_k , which stands for the update interval that is estimated for the target UE. The MSNN model may differ from one AP to another, due to the different locations and coverage areas. Specifically, the WiFi AP covers a much larger area than the LiFi AP, resulting in distinctive demands for the update interval. Though the LiFi APs have the same coverage area, their locations are different, which can also lead to variations in the required update interval. For this reason, the APs are classified into several types, and each type employs a dedicated MSNN model.

Regarding the HLWNet in Fig. 1, there are three kinds of LiFi APs depending on their locations (which are divided by Areas A, B, and C), in addition to a single WiFi AP. Thus, the APs are classified into four types: AP Type I contains 4 LiFi APs $\langle 6, 7, 10, 11 \rangle$ located in Area A; AP Type II contains 8 LiFi APs $\langle 2, 3, 5, 8, 9, 12, 14, 15 \rangle$ located in Area B; AP Type III contains the remaining 4 LiFi APs $\langle 1, 4, 13, 16 \rangle$ located in Area C; and AP Type IV is the WiFi AP $\langle 17 \rangle$. It is worth noting that the AP classification is subject to the symmetry of network topology. As for an asymmetrical topology, each AP can be an individual type. In this paper, the MSNN model is trained for just one AP in each type, since the trained MSNN model can be directly applied to the other APs in the same type. In practice, each AP can implement its own MSNN model, for the purpose of generality.

A DNN structure is designed for MSNN to map the input $\mathbf{z}_k = [\gamma_k, \theta_k, v_k]$ to the output T_k , as shown in Fig. 2. Specifically, \mathbf{z}_k is fed to two fully connected hidden layers. Let N_{L1} denote the number of neurons in the first layer and N_{L2} for the second layer. In the first layer, the weight matrix and the bias vector are denoted by $\mathbf{W}_1 \in \mathbb{R}^{3 \times N_{L1}}$ and $\mathbf{b}_1 \in \mathbb{R}^{N_{L1}}$. Similarly, the weight matrix and the bias vector are $\mathbf{W}_2 \in \mathbb{R}^{N_{L1} \times N_{L2}}$ and $\mathbf{b}_2 \in \mathbb{R}^{N_{L2}}$ for the second layer. The activation function adopted for the hidden layers is a rectified linear unit (ReLU), which is defined as $f_{\text{R}}(\mathbf{x}) = \max(0, \mathbf{x})$. In the output layer, the weight matrix and the bias vector

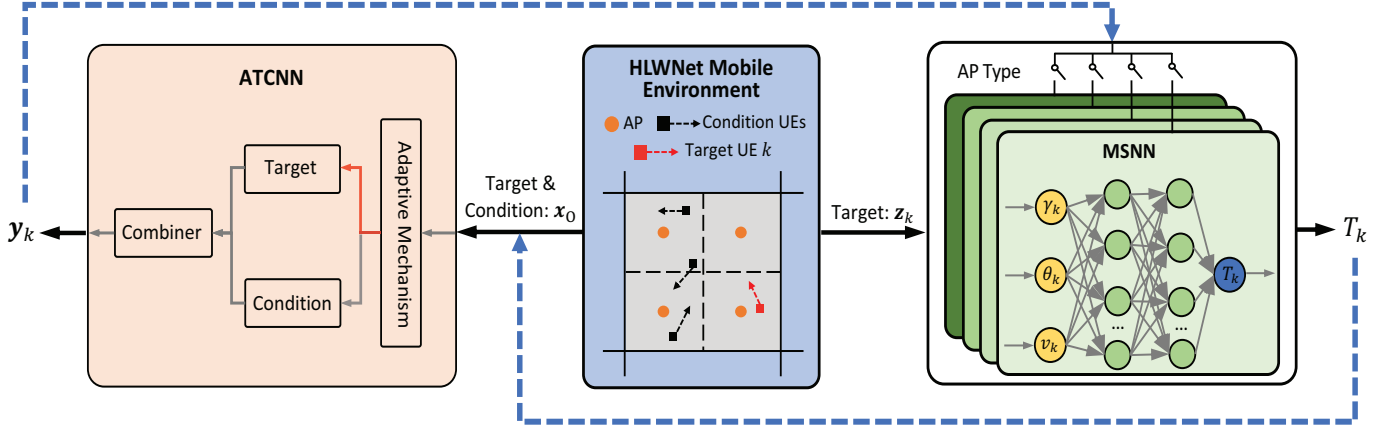


Fig. 2. Schematic diagram of the proposed MS-ATCNN (solid lines: information flow; dashed lines: control flow).

are denoted by $\mathbf{W}_3 \in \mathbb{R}^{N_{L2} \times 1}$ and $\mathbf{b}_3 \in \mathbb{R}^1$, respectively. Afterwards, the sigmoid activation function is used, which is defined as $f_S(\mathbf{x}) = 1/(1 + e^{-\mathbf{x}})$. Finally, the MSNN model outputs the estimated update interval T_k as follows:

$$T_k = f_S(\mathbf{W}_3 f_R(\mathbf{W}_2 f_R(\mathbf{W}_1 z_k + \mathbf{b}_1) + \mathbf{b}_2) + \mathbf{b}_3). \quad (3)$$

B. Framework of MS-ATCNN

Fig. 2 outlines the framework of MS-ATCNN, which consists of three key components: i) the MSNN model, ii) the ATCNN model, and iii) the mobile environment of an HLWNet. For a certain target UE, MS-ATCNN runs the resource and mobility management in a loop, which involves four steps.

- In the first step, information about the UEs is extracted from the mobile environment and fed to the ATCNN model. For UE j , the information is denoted by $\mathbf{x}_j = [\gamma_{1,j}, \gamma_{2,j}, \dots, \gamma_{N_a,j}, R_j]$, which is comprised of the SNR values and the required data rate. The overall information is denoted by $\mathbf{x}_O = [\mathbf{x}_1, \mathbf{x}_2, \dots, \mathbf{x}_k, \dots, \mathbf{x}_{N_u}]$, which contains the relevant information on both the target UE k and the other UEs (which are referred to as condition UEs) in the mobile environment.
- In the second step, the ATCNN determines the host AP for the target UE, upon the information it receives. As shown in Fig. 2, the ATCNN model consists of four function blocks: i) an adaptive mechanism to map any smaller number of UEs to a preset number; ii) a target neural network to extract the features of the target UE; iii) a condition neural network to extract the features of the condition UEs; and iv) a combiner neural network to make an LB solution for the target UE. See details about the ATCNN model in our previous work [17]. The output of ATCNN is denoted by \mathbf{y}_k , which indicates the host AP for the target UE. If \mathbf{y}_k differs from the previous result, the UE will be handed over to a new host AP; otherwise, the UE will stay with the current host AP until the next implementation of ATCNN.
- In the third step, the MSNN model is run to decide an update interval for the target UE. Upon the latest result

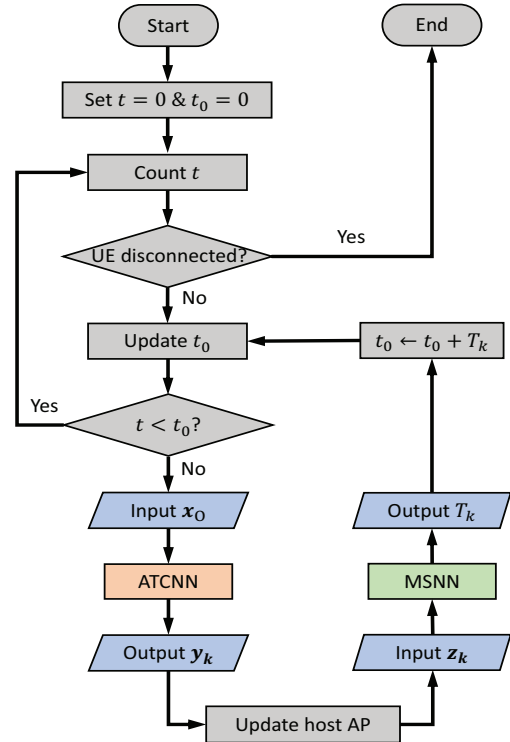


Fig. 3. Flowchart of the proposed MS-ATCNN.

from ATCNN, the corresponding AP implements its own MSNN. As mentioned, there are four types of APs in the considered HLWNet. Therefore, Fig. 2 presents a switch among four MSNN models, for illustration purposes. The MSNN model also acquires information from the mobile environment. Details about the MSNN model have been introduced in the previous subsection.

- In the last step, the output of the MSNN model (i.e., the update interval) is used to control when the ATCNN model is implemented for the next time. This is realised through controlling the information flow that is fed to ATCNN, i.e., the first step.

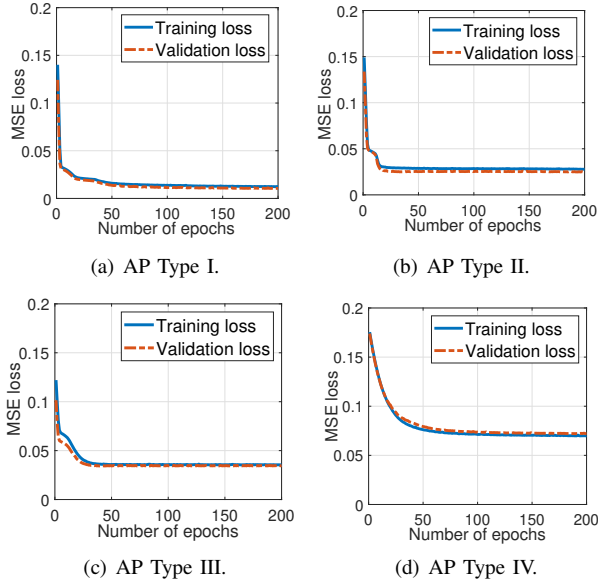


Fig. 4. Training loss and validation loss of the MSNN model.

Fig. 3 presents the flowchart of the proposed MS-ATCNN framework. In summary, the ATCNN model copes with the resource management, while the MSNN model handles the mobility management. The two models interact with each other, forming the concept of MS-ATCNN. Since the MS-ATCNN scheme enables an independent operation for each individual UE, adaptive update intervals are realised among the UEs, allowing them to tackle the resource and mobility management in a more flexible way than the conventional network-centric LB methods.

C. Dataset Collection

To train the proposed MSNN model, it is necessary to collect sample data of the update interval under a certain criterion. Since throughput is the key metric to measure the effectiveness of LB, we introduce a throughput-degradation criterion to obtain the ground-truth labels of update interval, which allows the throughput of the target UE to drop by a certain percentage against the ideal case with an infinitesimal update interval. This throughput-degradation percentage is denoted by Gap . For practical implementations, the ideal ATCNN is defined as running the ATCNN model at a fixed update interval of 10ms, considering the channel coherence time in HLWNets.

Let $\mathbf{y}_k^{(t)}$ denote the output of ATCNN at time t . Let t_0 denote the reference point of time. Assume that the ATCNN model is implemented at t_0 , and the output $\mathbf{y}_k^{(t_0)}$ is applied to the target UE until t_1 . Based on (2), the average throughput during this period can be calculated by:

$$\Gamma_k^{t_0 \rightarrow t_1}(\mathbf{y}_k^{(t_0)}) = \frac{1}{t_1 - t_0} \int_{t_0}^{t_1} \left(\sum_{i \in \mathcal{S}} \rho_{i,j}^{(t)} \chi_{i,j}^{(t_0)} C_{i,j}^{(t)} \right) dt. \quad (4)$$

Let \hat{T}_k denote the desired update interval. The average throughput resulted by MS-ATCNN can be expressed as $\tilde{\Gamma}_k^{t_0 \rightarrow \hat{T}_k}(\mathbf{y}_k^{(t_0)})$. During the same period, the ideal ATCNN

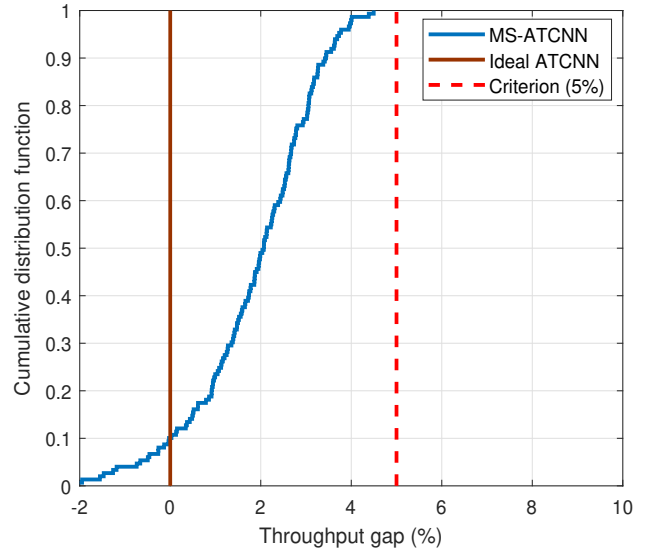


Fig. 5. Throughput gap between MS-ATCNN and ideal ATCNN.

updates its output every 10ms. Thus, the average throughput achieved by the ideal ATCNN can be computed by:

$$\tilde{\Gamma}_k^{t_0 \rightarrow \hat{T}_k} = \frac{1}{M} \sum_{m=1}^M \Gamma_k^{t_0 \rightarrow t_0 + \Delta t}(\mathbf{y}_k^{(t_0)}), \quad (5)$$

where Δt is 10ms for the defined ideal ATCNN and $t = t_0 + (m-1)\Delta t$, while M is the integer division between \hat{T}_k and Δt . Following the throughput-degradation criterion, the desired update interval \hat{T}_k can be obtained by satisfying:

$$\Gamma_k^{t_0 \rightarrow \hat{T}_k}(\mathbf{y}_k^{(t_0)}) = Gap \times \tilde{\Gamma}_k^{t_0 \rightarrow \hat{T}_k}. \quad (6)$$

The value of Gap is set to be 5% in this paper, to let the proposed MS-ATCNN achieve a satisfactory throughput performance, while allowing a certain extent of flexibility in terms of the update intervals.

D. Training, Validation and Test

1) *Training and Validation*: Following the above criterion, 2000 samples are collected to train the MSNN model of each AP type. The dataset is pre-processed with a linear normalisation, before it is fed into the MSNN model with a ratio of 80:20 between training data and validation data. The loss function is mean square error (MSE), which is commonly used for regression tasks in machine learning. The MSE loss function can be expressed as follows:

$$L_{\text{MSE}}(\alpha) = \frac{1}{N} \sum_{n=1}^N (T_{k,n} - \hat{T}_{k,n})^2, \quad (7)$$

where α denotes the set of all the weight matrices and bias vectors in the MSNN model; N is the number of samples; $T_{k,n}$ stands for the estimated update interval for UE k in the i -th sample; and $\hat{T}_{k,n}$ denotes the corresponding ground-truth label. The adaptive moment estimation (Adam) [26] is employed to train the MSNN model by iterating α through

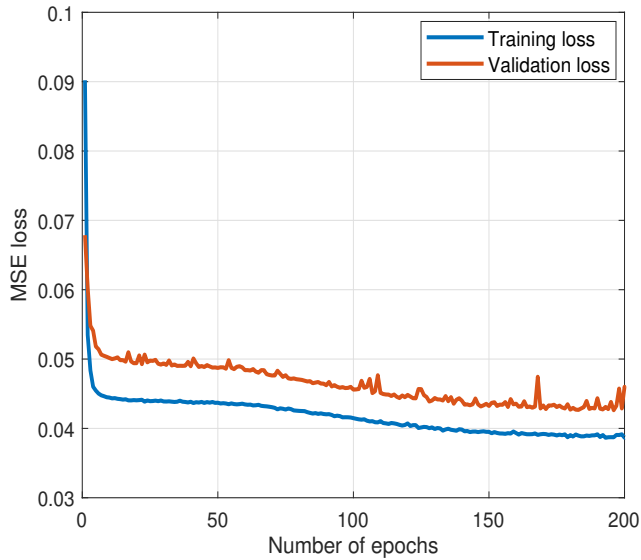


Fig. 6. Training loss and validation loss of MSNN without AP classification.

$\alpha \leftarrow \alpha - \eta \nabla L_{\text{MSE}}(\alpha)$, where η is the learning rate, and $\nabla L_{\text{MSE}}(\alpha)$ stands for the gradient of the loss function with respect to α . See details about the setup of the training parameters in Section V.

Fig. 4 presents the training loss and validation loss of the MSNN model for different AP types. In all cases, the validation loss matches the training loss closely, indicating that the MSNN model is adequately trained with no evident over-fitting or under-fitting phenomena. It is worth noting that the steady-state loss of AP Type IV (i.e., the WiFi AP) in Fig. 4(d) is noticeably higher than that of the other AP types (i.e., the LiFi APs) in Fig. 4(a)-4(c). This is mainly because the WiFi AP has a larger coverage area than the LiFi AP, leading to a less accurate training outcome. Apart from that, the convergence rates are slightly different among the AP types. On average, it requires around 50 epochs to reach a steady state.

2) *Test*: To verify the training performance of the MSNN model, we analyse the cumulative distribution function (CDF) of the throughput gap between MS-ATCNN and the ideal ATCNN, which is defined in Section III-C. The results are collected through 200 simulations with each lasting for 10s. Note that the ground-truth update intervals might be very long for slow-moving UEs, even exceeding the duration of simulations. For practical implementations, the ground-truth update intervals are capped at 2s.

As shown in Fig. 5, the throughput gap of MS-ATCNN is well below the preset throughput-degradation criterion, which is 5%. In fact, the average throughput gap is just around 2%. This is because capping the ground-truth update interval alleviates the degradation in throughput. It is also observed that the throughput gap of MS-ATCNN has a 10% probability of being negative. In other words, MS-ATCNN occasionally achieves a higher throughput than the ideal ATCNN. The reason is that the objective of ATCNN is to maximise the overall network throughput with a proportional fairness, rather

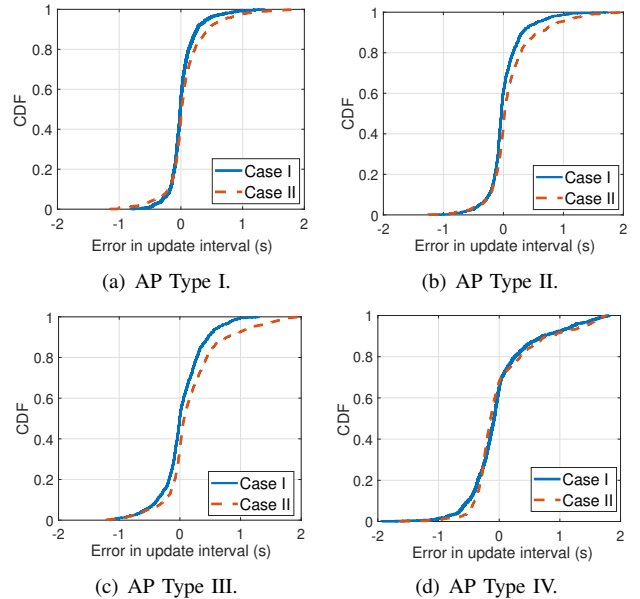


Fig. 7. Accuracy of the MSNN models with AP classification (Case I) and without AP classification (Case II).

than the throughput of the target UE. For certain scenarios, it is possible that MS-ATCNN with a longer update interval achieves a higher throughput than the case with a shorter update interval. For instance, when the target UE is moving towards its current host AP, the ATCNN model might transfer the UE to another AP that is further away, from the angle of balancing the overall network data traffic. With a longer update interval, the UE can stay with its current host AP and benefit from a higher throughput, at the cost of compromising the throughput performance of other UEs.

IV. ABLATION STUDY

In this section, two ablation studies are implemented to verify the effectiveness of the proposed MSNN model. The first one is examining the necessity of using dedicated MSNN models for different AP types. The second one is analysing the impact of each input variable on the MSNN model. The simulation setup is the same as in Section V.

A. Removal of AP Classification

As mentioned in Section III-A, the APs of the considered HLWNet are classified into four types, and each AP type is associated with a dedicated MSNN model. To verify the necessity of this implementation, we analyse the training performance of the MSNN model without AP classification, where the sample datasets of all AP types are mixed for training the model. Fig. 6 shows the training and validation losses in this case. As shown, the validation loss is noticeably higher than the training loss, indicating that the MSNN model is over-fitted without AP classification. By comparing Fig. 6 with Fig. 4, it can be concluded that AP classification can effectively eliminate the over-fitting issue in the training process of the MSNN model. The reason has been explained in Section III-A.

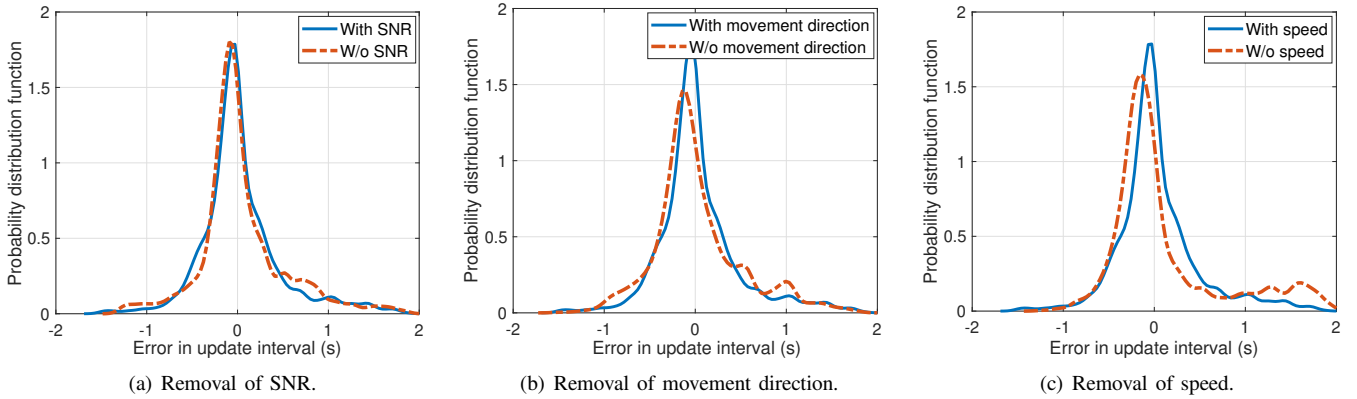


Fig. 8. Accuracy of the MSNN models with and without individual input variables.

Apart from the training loss, accuracy is also a key metric to measure the performance of a learning model. Here the accuracy is evaluated by the errors between the estimated update intervals and the ground-truth labels. Fig. 7 presents the CDF of those errors for the MSNN models with and without AP classification. In general, AP classification makes the MSNN model more accurate for the LiFi AP types (i.e., AP Type I, II and III). As shown, the MSNN models that are dedicated to those types are noticeably closer to zero than the case without AP classification. As for the WiFi AP (i.e., AP Type IV), the two cases exhibit similar levels of accuracy. This is because the WiFi AP covers a larger area than the LiFi AP, leading to a less accurate estimation of the update interval. Consequently, the samples of the WiFi AP dominate the accuracy of the MSNN model when it is trained with the mixed samples of different APs.

B. Removal of Individual Input Variables

We now analyse the accuracy of the MSNN models with and without individual input variables. Fig. 8(a) shows that when SNR is removed from the input, the error variance of MSNN increases from 0.200 to 0.226. Given a confidence level 80%, the proposed MSNN model obtains a confidence interval (CI) of errors within $[-406\text{ms}, 576\text{ms}]$, which is 11.5% smaller than the range $[-412\text{ms}, 697\text{ms}]$ offered by the case without SNR. These results signify that involving SNR as an input can help MSNN achieve a higher accuracy. Similarly, when the movement direction is removed from the input, the error variance of the MSNN model increases to 0.236, while the corresponding CI is enlarged to $[-479\text{ms}, 730\text{ms}]$, as shown Fig. 8(b). A similar but more pronounced trend can be found in the case of removing the variable speed, where the error variance soars to 0.381, as shown in Fig. 8(c). Meanwhile, the corresponding CI becomes $[-417\text{ms}, 1252\text{ms}]$, which is 70% larger than the proposed MSNN model. In summary, the three input variables (especially the UE's speed) are effective in delivering an accurate estimation of the update interval.

V. SIMULATION RESULTS

In this section, Monte Carlo simulations are carried out to evaluate the performance of the proposed MS-ATCNN.

 TABLE II
PARAMETER SETUP

HLWNet Parameters	Values
Room size, $L \times W \times H$	10m×10m×3m
Number of LiFi APs	16
Number of WiFi APs	1
LiFi AP separation	2.5 m
UE height	0.5 m
Number of UEs	[10, 100]
Average data rate requirement	100 Mbps
Other LiFi and WiFi parameters	Refer to [17]
Dataset Collection Parameters	Values
Throughput-degradation percentage, Gap	5%
Range of movement direction	$[0, 2\pi]$
Range of speed	$(0, 10]$ m/s
Sample number per AP type, N	2000
Duration per sample, T	10 s
Training Parameters	Values
Number of hidden neurons, N_{L1}	16
Number of hidden neurons, N_{L2}	4
Loss function	MSE
Learning rate, η	0.00001
Optimiser	Adam

Three baseline methods are taken into account: i) ATCNN with different update schemes other than the MSNN model; ii) GT [11], a conventional network-centric LB method; and iii) SSS, a straightforward AP selection method without the capability of LB. The simulations are carried out in Python3.8 on a desk computer with an Intel Core i5-10500@3.1GHz processor, with the parameters summarised in Table II. The relevant codes are open-sourced in [27].

A. MS-ATCNN versus ATCNN

In this subsection, the throughput performance of MS-ATCNN is compared with ATCNN to verify the effectiveness of the proposed mechanism, i.e., adaptive update interval. To guarantee a fair comparison, we let ATCNN adopt the same amount of average update interval as MS-ATCNN, of which the measured results are given in Table III. This case is referred to as ATCNN@Aver. Two other cases of ATCNN are also considered: i) with a certain fixed update interval (e.g.,

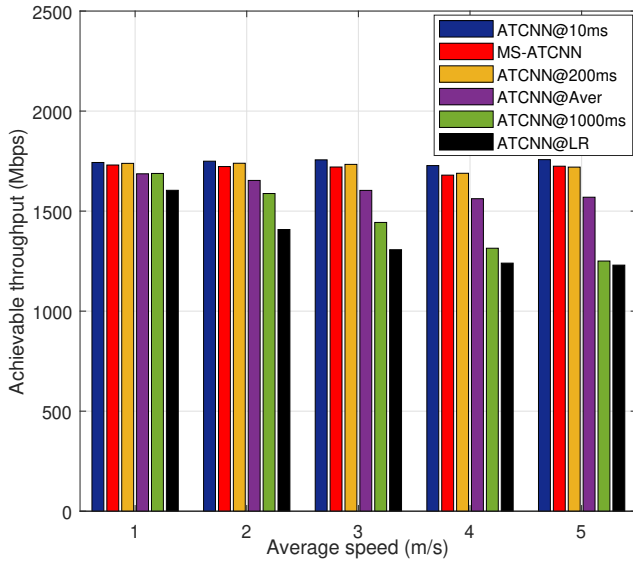


Fig. 9. Network throughput versus the UEs’ average speed, compared to ATCNN with different update schemes ($N_u = 50$).

TABLE III
AVERAGE UPDATE INTERVAL OF MS-ATCNN.

Average speed (m/s)	1	2	3	4	5
Average update interval (ms)	1014	742	626	490	443

ATCNN@10ms), ii) using a linear regression (LR) model to yield the update interval in accordance to the UE’s speed¹. The later case is referred to as ATCNN@LR. The impact of algorithm runtime is not involved here but will be analysed in the following subsections.

Fig. 9 presents the overall network throughput achieved by MS-ATCNN, against ATCNN with different update schemes that are described above. Among all the schemes, ATCNN@10ms exhibits the highest throughput, as expected. Due to the lag effect, the throughput performance of ATCNN drops as the update interval increases, especially in the case of a higher UE speed. Also, it is observed that MS-ATCNN achieves a throughput comparable to ATCNN@200ms, while the average update interval of MS-ATCNN is much longer than 200 ms, resulting in a lower feedback cost. Compared to ATCNN@Aver, which employs the same amount of average update interval as MS-ATCNN, the later gains a noticeable throughput increase. Taken 5 m/s as an example, MS-ATCNN obtains a throughput of 1,740 Mbps, which is 10.1% higher than the 1,580 Mbps achieved by ATCNN@Aver. Further, it proves that MSNN is more effective than the LR model, which is an intuitive adaptive update scheme. As can be seen, the throughput gap between MS-ATCNN and ATCNN@LR increases with the UEs’ average speed, from 8.0% at 1 m/s to 39.2% at 5 m/s.

¹Two reference points in the format (speed, update interval) are adopted for the LR model: (1 m/s, 2 s) and (10 m/s, 0.01 s). The update interval for each UE is determined by its speed. For example, the resulted update interval is 1.8 s for 1 m/s and 1 s for 5 m/s, respectively.

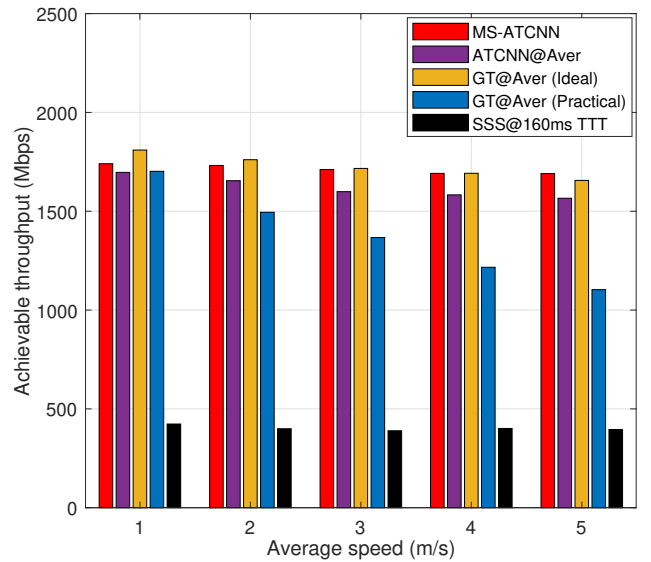


Fig. 10. Network throughput versus the UEs’ average speed, compared to GT and SSS ($N_u = 50$).

B. MS-ATCNN versus Network-Centric Load Balancing

In this subsection, we focus on comparing the throughput performance of MS-ATCNN with GT, which is a typical network-centric LB method. Similar to ATCNN@Aver, GT uses the same amount of average update interval as MS-ATCNN, in order to ensure a fair comparison. Accordingly, this method is referred to as GT@Aver. It is worth noting that GT requires a substantial amount of runtime, which would cause a lag effect and degrade the throughput performance. Therefore, two cases of GT are considered: the ideal case and the practical case, depending on whether the impact of runtime is taken into account. In contrast to GT, MS-ATCNN costs an ultra-low runtime, which is negligible in relation to the channel coherence time. Thus, the throughput results of MS-ATCNN with and without the impact of runtime are physically the same. For this reason, only the results of MS-ATCNN with the impact of runtime are presented here. In addition to GT, SSS in association with a standard handover process (which has a TTT of 160 ms [28]) is also involved. This approach offers a baseline from two perspective: i) SSS itself exhibits the network capacity without the capability of LB, providing a comparison with MS-ATCNN in terms of resource management; and ii) the user-centric handover scheme renders a comparison with MS-ATCNN in regards to mobility management.

1) *Impact of the UEs’ Average Speed:* Fig. 10 presents the achievable throughput of MS-ATCNN against the above baseline methods for different values of the UEs’ average speed. As shown, the achievable throughput of MS-ATCNN is comparable to that of GT@Aver (Ideal). However, when involving the practical algorithm runtime, MS-ATCNN can significantly outperform GT@Aver (Practical), especially in a highly mobile environment. It is also found that the network throughput of MS-ATCNN reduces very slightly as the UEs move faster. When the UEs’ average speed increases from 1

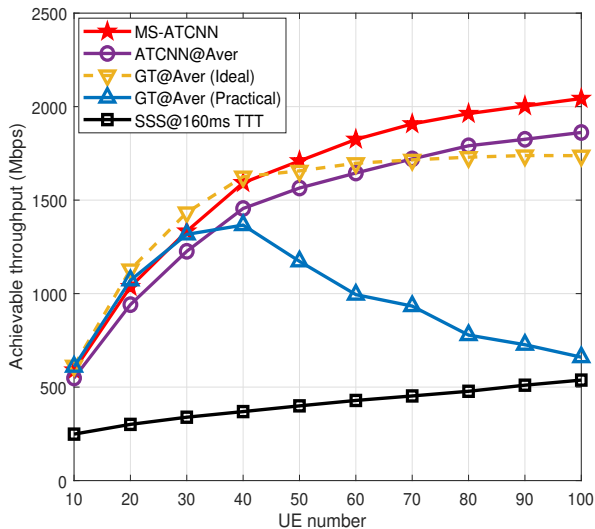


Fig. 11. Network throughput versus the number of UEs ($\bar{v} = 5$ m/s).

m/s to 5 m/s, the throughput obtained by MS-ATCNN reduces from 1,750 Mbps to 1,690 Mbps. In contrast, GT@Aver (Practical) exhibits a prominent decrease in throughput from 1,700 Mbps to 1,100 Mbps. Accordingly, the throughput gain achieved by MS-ATCNN against GT@Aver (Practical) enlarges from 2.9% to 59.1%. The reason behind this trend is that MS-ATCNN costs a much lower amount of runtime than GT. See a detailed analysis of the algorithm runtime in Section V-C. Despite with user-centric handover, the throughput performance of SSS is far worse than the others, due to the lack of LB capability. Taken 5 m/s as an example, MS-ATCNN acquires a network throughput 322.5% higher than SSS.

2) *Impact of the Number of UEs*: Fig. 11 presents the network throughput as a function of the number of UEs N_u , with the UEs' average speed \bar{v} set to be 5 m/s as an example. Three outcomes are observed. First, the achievable throughput increases with N_u for all the involved methods, except GT@Aver (Practical). This is because the runtime of GT drastically increases with N_u , which will be discussed in the following subsection. Accordingly, the throughput gap between GT@Aver (Ideal) and GT@Aver (Practical) enlarges from 0% to 62.2% when N_u increases from 10 to 100. Second, the network throughput of MS-ATCNN slightly falls behind that of GT@Aver (Ideal) when $N_u \leq 45$, but the situation is opposite for a larger N_u . The reason for this trend is two-fold. On the one hand, the ATCNN model is trained with the dataset collected from GT, leading to an inevitable throughput gap, as discussed in [17]. On the other hand, MS-ATCNN benefits from its unique adaptive update scheme, in comparison to the fixed update scheme for GT. For a smaller N_u , the former factor dominates and hence the throughput of MS-ATCNN is marginally lower than that of GT@Aver (Ideal). While N_u becomes larger, the latter factor dominates and thus MS-ATCNN surpasses GT@Aver (Ideal) in terms of throughput. Third, as N_u increases from 10 to 100, MS-ATCNN achieves almost the same throughput as GT@Aver (Practical) at first until N_u reaches 30, but afterwards the

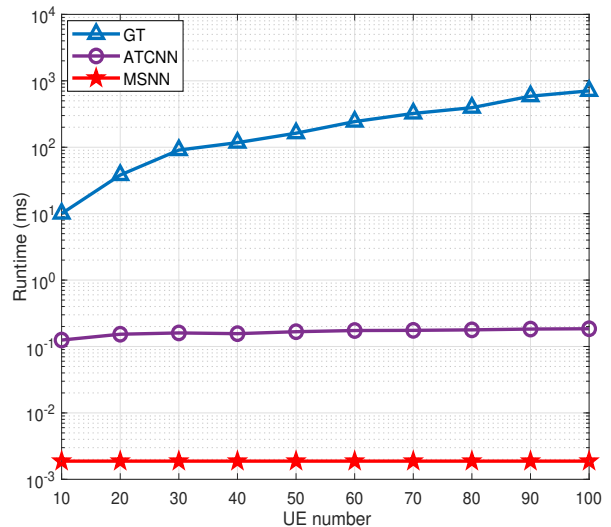


Fig. 12. Algorithm runtime versus the number of UEs.

throughput gap between the two methods increases promptly, leading to a gain of 215% by MS-ATCNN when $N_u = 100$. This trend is a combined effect of the previous two outcomes.

C. Analysis of Computational Complexity

As mentioned before, the computational complexity of an LB method can have a non-negligible impact on its network performance. The Big-O complexity of GT can be expressed as $\mathcal{O}(N_a N_u I_{GT})$ [11], where I_{GT} is the number of iterations required by GT. The complexity of MS-ATCNN is a sum of that of ATCNN and MSNN. The Big-O complexity of implementing ATCNN is $\mathcal{O}(N_a M K_m + K_o)$ [17], where M denotes the maximum number of UEs that ATCNN can support (in this paper $M = 100$); $\mathcal{O}(K_m)$ is the complexity of additions and multiplications in the FC layers; and $\mathcal{O}(K_o)$ is the complexity of other operations including the BN and activation functions. As for MSNN, its Big-O complexity is $\mathcal{O}(N_{L_1} N_{L_2})$, which is a constant value regarding different UE numbers.

Fig. 12 shows the runtime as a function of the number of UEs for MSNN, ATCNN and GT, with the same configuration in MATLAB R2022b to provide a fair comparison. It is observed that the runtime of MSNN is two orders of magnitude lower than that of ATCNN. Specifically, MSNN costs a runtime around 2 μ s, regardless of N_u . This matches the fact that MSNN only involves a single target UE. As for ATCNN, its runtime slightly increases with N_u , ranging between 120 μ s and 184 μ s. Thus, ATCNN plays a dominant role in the runtime of MS-ATCNN. In contrast, GT consumes a significant amount of runtime, which exhibits a prominent increase from 10 ms to 700 ms when N_u increases from 10 to 100. The runtime of GT is about 80 times that of MS-ATCNN when $N_u = 10$, and this gap soars to 3,800 times when $N_u = 100$.

VI. CONCLUSION

In this paper, a novel user-centric learning method named MS-ATCNN was proposed to tackle the joint resource and mobility management issue for hybrid networks such as HLWNets. The proposed MS-ATCNN consists of two key components: i) the ATCNN model which makes the LB solution for a target UE, from the perspective of resource management; and ii) the MSNN model which decides when the ATCNN model is implemented the next time, from the perspective of mobility management. Unlike the conventional network-centric LB schemes which can only be updated for all the UEs at the same pace, MS-ATCNN enables adaptive update frequencies among the UEs in accordance to their moving status. This is attributed to the unique feature of user-centric LB that resides in MS-ATCNN. Results show that with the same amount of average update interval, MS-ATCNN can significantly improve the network throughput against the conventional LB methods such as GT, with an increase up to 215%. Apart from that, MS-ATCNN only requires a runtime at the level of 100s μ s, which is two to three orders of magnitude lower than GT. For these reasons, MS-ATCNN can facilitate achieving highly efficient spectrum aggregation in hybrid networks, delivering great potential to meet the requirements of future wireless communications.

REFERENCES

- [1] C.-X. Wang, X. You, X. Gao, X. Zhu, Z. Li, C. Zhang, H. Wang, Y. Huang, Y. Chen, H. Haas *et al.*, "On the road to 6G: Visions, requirements, key technologies and testbeds," *IEEE Commun. Surv. Tutor.*, 2023.
- [2] H. Haas, L. Yin, Y. Wang, and C. Chen, "What is LiFi?" *J. Lightw. Technol.*, vol. 34, no. 6, pp. 1533–1544, 2015.
- [3] F. Hu *et al.*, "Si-substrate leds with multiple superlattice interlayers for beyond 24 Gbps visible light communication," *Photonics Research*, vol. 9, no. 8, pp. 1581–1591, 2021.
- [4] W. Wu, "Performance analysis of visible light communications with channel blockage caused by human bodies," in *2023 IEEE Int. Conf. on Communications (ICC)*, 2023, pp. 1–5.
- [5] Y. Zhu, C. Gong, J. Luo, M. Jin, X. Jin, and Z. Xu, "Indoor non-line of sight visible light communication with a Bi-LSTM neural network," in *2020 IEEE Int. Conf. Commun. Workshops (ICC Workshops)*, 2020, pp. 1–6.
- [6] "Cisco annual internet report (2018–2023) white paper," *Cisco: San Jose, CA, USA*, vol. 10, no. 1, pp. 1–35, 2020.
- [7] X. Wu, M. D. Soltani, L. Zhou, M. Safari, and H. Haas, "Hybrid LiFi and WiFi networks: A survey," *IEEE Commun. Surv. Tutor.*, vol. 23, no. 2, pp. 1398–1420, 2021.
- [8] D. A. Basnayaka and H. Haas, "Hybrid RF and VLC systems: Improving user data rate performance of VLC systems," in *2015 IEEE 81st Veh. Technol. Conf. (VTC Spring)*, 2015, pp. 1–5.
- [9] Q. Ye, B. Rong, Y. Chen, M. Al-Shalash, C. Caramanis, and J. G. Andrews, "User association for load balancing in heterogeneous cellular networks," *IEEE Trans. Wirel. Commun.*, vol. 12, no. 6, pp. 2706–2716, 2013.
- [10] X. Li, R. Zhang, and L. Hanzo, "Cooperative load balancing in hybrid visible light communications and WiFi," *IEEE Trans. Commun.*, vol. 63, no. 4, pp. 1319–1329, 2015.
- [11] Y. Wang, X. Wu, and H. Haas, "Load balancing game with shadowing effect for indoor hybrid LiFi/RF networks," *IEEE Trans. Wireless Commun.*, vol. 16, no. 4, pp. 2366–2378, 2017.
- [12] S. Aboagye, T. M. Ngatched, O. A. Dobre, and A. Ibrahim, "Joint access point assignment and power allocation in multi-tier hybrid RF/VLC HetNets," *IEEE Trans. Wireless Commun.*, vol. 20, no. 10, pp. 6329–6342, 2021.
- [13] X. Wu, M. Safari, and H. Haas, "Access point selection for hybrid Li-Fi and Wi-Fi networks," *IEEE Trans. Commun.*, vol. 65, no. 12, pp. 5375–5385, 2017.
- [14] H. Ji and X. Wu, "A novel method of combining decision making and optimization for LiFi resource allocation," in *2022 IEEE Glob. Commun. Conf. Workshops (GC Wkshps)*, 2022, pp. 1616–1621.
- [15] A. M. Alenezi and K. A. Hamdi, "Reinforcement learning approach for hybrid WiFi-VLC networks," in *2020 IEEE 91st Veh. Technol. Conf. (VTC2020-Spring)*, 2020, pp. 1–5.
- [16] R. Ahmad, M. D. Soltani, M. Safari, and A. Srivastava, "Reinforcement learning-based near-optimal load balancing for heterogeneous LiFi WiFi network," *IEEE Syst. J.*, vol. 16, no. 2, pp. 3084–3095, 2021.
- [17] H. Ji, X. Wu, Q. Wang, S. J. Redmond, and I. Tavakkolnia, "Adaptive target-condition neural network: DNN-aided load balancing for hybrid LiFi and WiFi networks," *IEEE Trans. Wireless Commun.*, doi: 10.1109/TWC.2023.3339503.
- [18] Y. Wang and H. Haas, "Dynamic load balancing with handover in hybrid Li-Fi and Wi-Fi networks," *J. Lightw. Technol.*, vol. 33, no. 22, pp. 4671–4682, 2015.
- [19] L. Li, Y. Zhang, B. Fan, and H. Tian, "Mobility-aware load balancing scheme in hybrid VLC-LTE networks," *IEEE Commun. Lett.*, vol. 20, no. 11, pp. 2276–2279, 2016.
- [20] X. Wu and H. Haas, "Load balancing for hybrid LiFi and WiFi networks: To tackle user mobility and light-path blockage," *IEEE Trans. Commun.*, vol. 68, no. 3, pp. 1675–1683, 2020.
- [21] X. Wu, D. C. O'Brien, X. Deng, and J.-P. M. Linnartz, "Smart handover for hybrid LiFi and WiFi networks," *IEEE Trans. Wirel. Commun.*, vol. 19, no. 12, pp. 8211–8219, 2020.
- [22] X. Wu and D. C. O'Brien, "A novel machine learning-based handover scheme for hybrid LiFi and WiFi networks," in *2020 IEEE Glob. Comm. Conf. Workshops (GC Wkshps)*. IEEE, 2020, pp. 1–5.
- [23] G. Ma, R. Parthiban, and N. Karmakar, "An artificial neural network-based handover scheme for hybrid LiFi networks," *IEEE Access*, vol. 10, pp. 130 350–130 358, 2022.
- [24] X. Wu and H. Haas, "Mobility-aware load balancing for hybrid LiFi and WiFi networks," *J. Opt. Commun. Netw.*, vol. 11, no. 12, pp. 588–597, 2019.
- [25] D. B. Johnson and D. A. Maltz, "Dynamic source routing in ad-hoc wireless networks," *Mobile computing*, pp. 153–181, 1996.
- [26] D. P. Kingma and J. Ba, "Adam: A method for stochastic optimization," *arXiv preprint arXiv:1412.6980*, 2014.
- [27] H. Ji and X. Wu, "Resource and Mobility Management in Hybrid LiFi and WiFi Networks: A User-centric Learning Approach," Nov. 2023. [Online]. Available: <https://github.com/HanJi-UCD/MS-ATCNN>
- [28] "LTE: Evolved universal terrestrial radio access (E-UTRA); Radio resource control (RCC); Protocol specification (Release 13)," 3GPP TS 36.331 v13.0.0., Valbonne, France, Tech. Rep., Jan. 2016.